Limnol. Oceanogr., 53(5), 2008, 2007–2020

Physical processes and hypoxia in the central basin of Lake Erie

Yerubandi R. Rao[1]
Environment Canada, Water Science & Technology, National Water Research Institute, Canada Centre for Inland Waters, Burlington, Ontario L7R 4A6, Canada

Nathan Hawley
NOAA–Great Lakes Environmental Research Laboratory, 2205 Commonwealth Boulevard, Ann Arbor, Michigan

Murray N. Charlton and William M. Schertzer
Environment Canada, Water Science & Technology, National Water Research Institute, Canada Centre for Inland Waters, Burlington, Ontario L7R 4A6, Canada

Abstract

The circulation and exchange processes during summer stratification were examined using time-series data of horizontal velocity, temperature, and dissolved oxygen profiles during 2004 and 2005 in the mid-central basin of Lake Erie. The current and temperature spectra showed a prominent peak at around 18 h, indicating the presence of clockwise rotating inertial waves. The mean bottom currents were strong (>0.1 m s^{-1}) and flowed in opposite direction to winds because of the surface pressure gradient due to wind set-up. The general range of horizontal exchange coefficients in the central basin is 0.2–1.2 m^2 s^{-1}. Vertical exchange coefficients varied from 1×10^{-5} to 1×10^{-4} m^2 s^{-1}. The high values usually occurred in the surface layer because of surface winds. The source of turbulent energy is current shear due to near-inertial oscillations in and above the thermocline and shearing stress due to the effect of mean currents and wave-induced motions during energetic wind events at the lake bottom. During strong wind episodes significant wave-induced currents were observed close to the bottom. The short-term oxygen depletion rates varied considerably between +0.87 mg L^{-1} d^{-1} and -1.16 mg L^{-1} d^{-1} in 2004 mainly because of physical processes in the central basin. When the hypolimnion depth is sufficiently thick (4 m), short-term changes in dissolved oxygen concentrations were partly due to vertical mixing and partly due to horizontal transport and mixing.

About one-third of the total population of the Great Lakes basin resides within the Lake Erie watershed, so of all of the Great Lakes, Lake Erie is exposed to the greatest stress from urbanization, industrialization, and agricultural activities from both the United States and Canada. Eutrophication of the lake was of critical concern especially during the 1950s to the 1970s, resulting in excessive algal populations and the occurrence of hypolimnetic anoxic conditions in the central basin and embayments. High concentrations of phosphorus were deemed to be the main culprit (Vollenweider 1968). A comprehensive bi-national phosphorus reduction strategy was implemented to reduce phosphorus discharge from wastewater treatment plants and limit the use of phosphorus-containing detergents in the watershed, but the hoped-for elimination of low oxygen levels in the central basin hypolimnion (as stated in the Great Lakes Water Quality Agreement of 1977) has not occurred, and relatively large increases in nitrogen continue to be observed. Recently, a decrease in phosphorus concentrations observed in the mid-1990s has been reversed as concentrations have rebounded through 2000–2001 (Charlton and Milne 2004). The introduction of zebra mussels in the late 1980s triggered changes in aquatic habitat suitability and altered the food web dynamics, energy transfer, and cycling of nutrients and contaminants within the lake ecosystem.

The last major physical experiments conducted in Lake Erie were Project Hypo in 1970 (Burns and Ross 1972) and the Lake Erie Bi-National Investigation in 1979–1980 (documented in a special issue of the *Journal of Great Lakes Research*, Boyce et al. 1987). These were intensive investigations that resulted in better understanding of the dynamics of the lake thermal regime, circulation, and inter-basin transports applied to water quality problems in the lake. The recent application of water quality models suggest that simulations of nutrients are diverging from the observations, but the levels of dissolved oxygen are still reasonably calculated (Lam et al. 2002). This suggests that there may be very real effects that can be attributable to the influences, such as invasive species like zebra mussels and climate change.

Increased understanding of the mechanisms that affect the hypoxia issue in Lake Erie is required in order to provide options for lake management. There is a critical need for better estimates of water and nutrient retention coefficients, lake circulation, inter-basin exchanges, ther-

[1] Corresponding author (Ram.Yerubandi@ec.gc.ca).

Acknowledgments

National Water Research Institute and Great Lake Environmental Research Laboratory's Engineering services and Technical Operations supported us in deploying and retrieving the moorings. We thank R. Rowsel and J. Milne, NWRI, for processing the data. The comments of two anonymous reviewers and C. Rehmann improved the quality of the manuscript. This is GLERL contribution #1454.

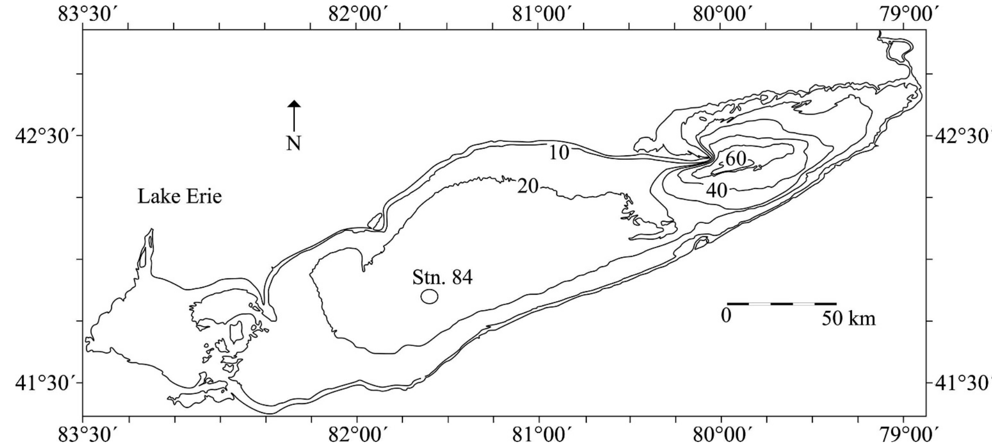

Fig. 1. Map of Lake Erie with the location of the mooring. Contour lines are in meters.

mal structure, and turbulent mixing. These are required to support further development of lake hydrodynamic, water quality, and ecosystem models for both diagnostic and prognostic examination of this problem. A multi-disciplinary team has been formed in the National Water Research Institute (NWRI) to address these issues. One of the goals of the program is to study the physical processes thought to be important to chemical and biological processes, particularly those involving vertical and horizontal exchanges in Lake Erie. In 2005, the International Field Years for Lake Erie (IFYLE) was established by the Great Lakes Environmental Research Laboratory (GLERL, a NOAA laboratory) to investigate the causes and consequences of hypoxia in the lake. Other parts of the GLERL program deal with harmful algal blooms and coupling lake physics with forecasts of fish production (Hawley et al. 2006). Extensive field observations were made in Lake Erie during the summers of 2004 and 2005 as part of these two programs.

The physical characteristics of the central basin of Lake Erie are sensitive to changes in meteorological conditions. Characteristics of seasonal temperature cycle in Lake Erie were described based on 1979–1980 data by Schertzer et al. (1987). During the stable summer stratification period they observed a very thin metalimnion at about 15–20 m. Ivey and Boyce (1982) analyzed temperature, velocity, and meteorological records for a brief period in summer and showed that the warming and thickening of the hypolimnion is due to turbulent entrainment of overlying metalimnion (thermocline) water into the hypolimnion. Ivey and Patterson (1984) used a one-dimensional model (Dynamic Reservoir Simulation Model; DYRESM) to describe the vertical mixing in the central basin. Saylor and Miller (1987) described large-scale currents in Lake Erie. Their observations showed a spectral peak at 18 h, indicating the presence of strong near-inertial oscillations in the thermocline currents. Boyce and Chiocchio (1987) studied water movements in the central basin and concluded that the observed features of the circulation could be related to the role of stratification in governing the vertical distribution of turbulent mixing. Royer et al. (1987) used the same set of measurements to track the short-term physical and biological changes in Lake Erie. Because of the success of several one-dimensional thermocline models, several researchers treated the heat budget of the central basin as a one-dimensional (vertical) problem (Ivey and Patterson 1984; Lam and Schertzer 1987). However, all of these studies concluded that the vertical sampling of currents, particularly in the epilimnion, and temperature was insufficient to resolve the details of the coupling of physical and biochemical structure in the lake. The data collected during the summers of 2004 and 2005 offer the opportunity to carry out a detailed analysis of circulation and mixing at a location in the mid-central basin. The main objectives of this article are then to study the variability and dynamics of currents and to calculate horizontal and vertical mixing characteristics in the mid-central basin in Lake Erie during the summer stratified season. We use this information to understand the physical processes that affect dissolved oxygen concentration in the hypolimnion.

Experimental data

During the summer stratified period from July to October 2004 an extensive field measurement program was undertaken by NWRI in all three basins of Lake Erie (Fig. 1). As a part of this field program, one 1200-KHz narrowband ADCP by RD Instruments was deployed at Sta. 84 in the central basin (41°56′06′′N, 81°39′44′′W, water depth = 24.5 m). Time series measurements of current profiles were also made at this station from April to October 2005 by a 300-KHz broadband Acoustic Doppler Current Profiler (ADCP) as a part of the IFYLE program. Hourly velocity profiles were obtained at 1-m intervals from 22 m to 2 m in 2004 and 19 m to 3 m in 2005. The data screening procedures used ensures data quality and utilizes processing parameters in which the error velocity is <0.01 m s^{-1} before temporal averaging. In addition to the ADCP, near-bottom currents were also obtained by a Sontek Hydra single-point current meter at 0.75 m above the bottom in 2004. All of the sensors were placed on the bottom looking upward. Temperature profiles were obtained from thermistor strings located close to ADCP stations. Data were recorded every 2 m at 30-minute intervals. The accuracy of temperature data is in the order of 0.1°C.

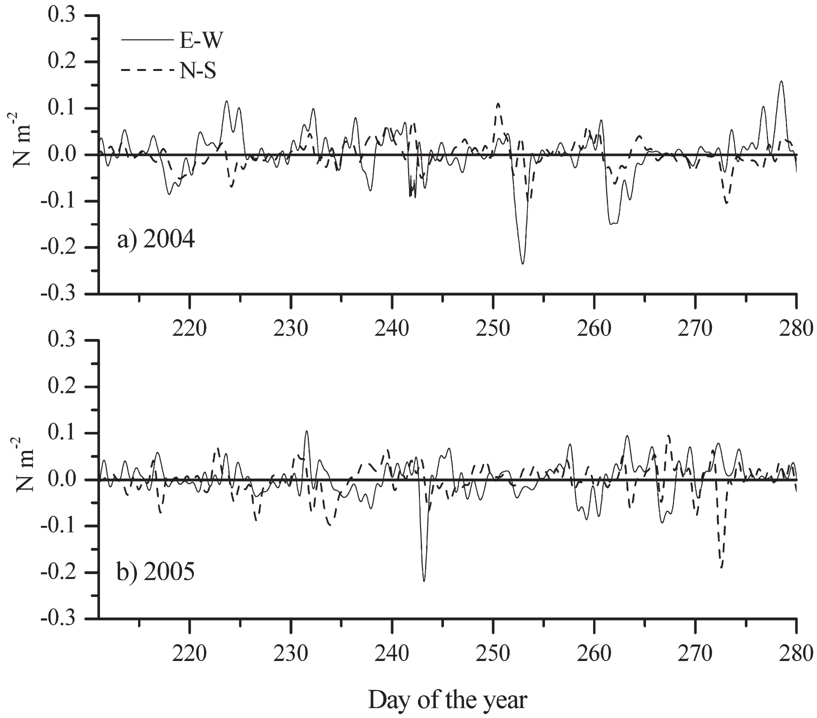

Fig. 2. Time series of the components of low-pass filtered (>24 h) wind stress at the central basin mooring during the summers of (a) 2004 and (b) 2005.

Wind observations

Currents in the lake are determined mainly by the winds over the lake. Meteorological buoys with observations of air temperature, wind speed and direction, relative humidity, and solar radiation were deployed at this location in both 2004 and 2005. The wind stress was obtained from the quadratic law given as $\tau = \rho_a C_d |W| W$, where $\rho_a = 1.2$ kg m^{-3} is the air density and W is wind velocity. In general, drag coefficient C_d increases with the wind speed and is estimated as $C_d = (0.8 + 0.065\ W) \times 10^{-3}$ for $W > 1$ m s^{-1} (Wu 1980). Here, the direction of wind stress points toward the reference.

In both years the winds were generally moderate (average speed was 4.5 m s^{-1}) and fluctuated between east and west with a typical period of 3–4 days. A low-pass filter, using a 24-h period for the cut-off, was used to remove the high-frequency information in the wind stress (Fig. 2a,b). The filtered time series has peaks of more than 0.2 N m^{-2} during the summer of 2004 associated with easterly winds on days 252 and 261. Toward the end of the summer the predominant wind direction was from the east. Another moderate event occurred toward the end of the summer on day 272. Although during 2005 several moderate westerly and northerly events were observed, the major wind event (0.23 N m^{-2}) occurred from days 241 to 242. During this period the winds were mainly northeasterly. Another northerly wind event occurred toward the end of the deployments.

Thermal structure and currents

A time series of temperature and horizontal velocity profiles are used to describe the variability of thermal structure and circulation from day 211 to day 280 in 2004 and 2005 (Fig. 3a,b). In 2004 two thermistors situated at 17 m and 18 m failed to provide good data. Therefore, a cubic spline technique was used to interpolate temperatures at these depths. The thermal structure in 2004 shows a strong stratification and a very sharp thermocline between 15 m and 20 m from day 211 to day 262. Some wind events occurred throughout the period, affecting the temperature of the upper layer. During days 252–253 strong easterly wind depressed

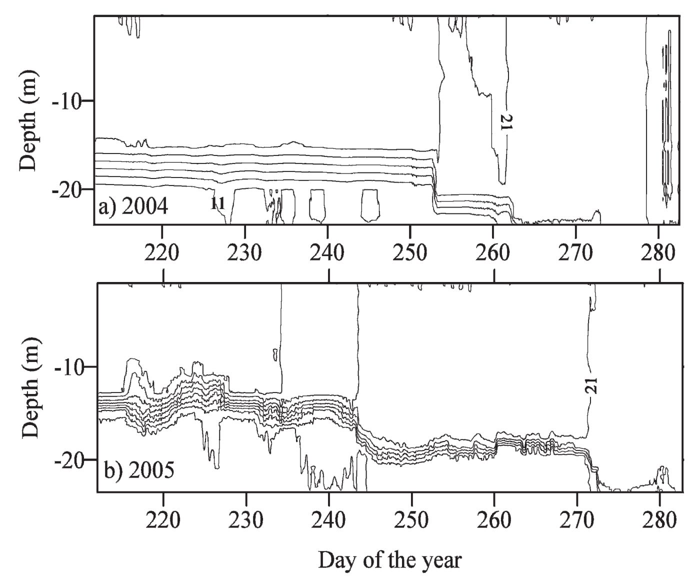

Fig. 3. The time series of vertical temperature distributions during the summers of (a) 2004 and (b) 2005.

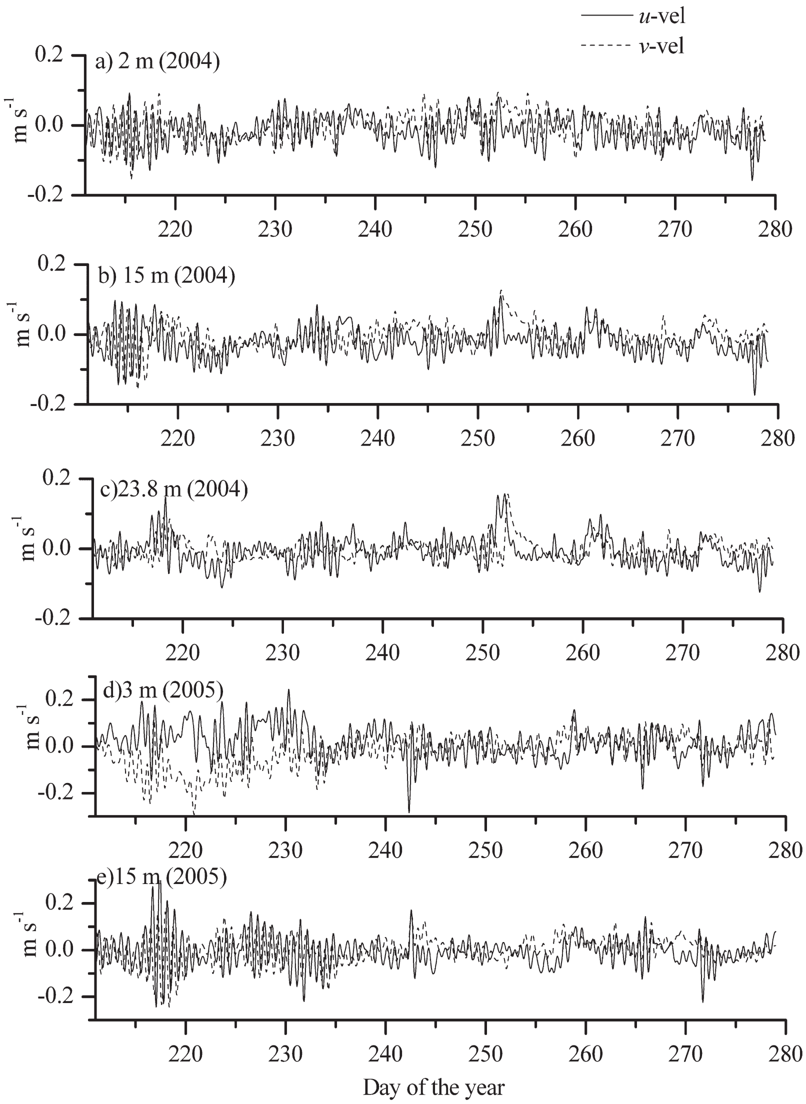

Fig. 4. The time series of low-pass filtered (>8 h) east–west (+ve to the east) and north–south (+ve to the north) components for selected ADCP bins in 2 years: (a) 2 m (2004), (b) 15 m (2004), (c) 23.8 m (2004), (d) 3 m (2005), and (e) 15 m (2005).

the thermocline by 4 m, and by day 258 the thermocline was close to the bottom. Between this period and the complete overturn on day 264 the thickness of the hypolimnion decreased significantly. From day 264, the combined effects of radiative and turbulent heat losses and high winds effectively broke down the thermal stratification. During 2005 the lake was significantly warmer than in 2004. This could be due to fewer high wind events and warmer weather, for example air temperature in 2005 is 3°C higher than in 2004. In 2005, the thermocline was not as deep compared to 2004. The top of the hypolimnion was at approximately 17–18 m from day 211 to 236. Within this period, as observed in 2004, thermocline water mixed with the hypolimnion because of strong wind events on two occasions. For example, a strong wind event on day 242 depressed the thermocline by 5 m and it remained there until the overturn on day 272.

The variability of filtered current time series at selected depths during the summers of 2004 and 2005 is shown in Fig. 4. The east–west currents were marginally higher than the north–south components, in accord with previous observations in Lake Erie (Saylor and Miller 1987). East–west wind and current variations in the east–west direction tend to be somewhat correlated in the surface layer; however, episodes of strong easterly winds generate a return flow and induce large bottom currents near the bottom. This indicates that the currents at this location respond directly to, and are affected by, pressure gradient setup by large-scale variations of the surface winds. At the bottom (Fig. 4c), low-pass filtered currents were strong (e.g., >0.1 m s^{-1}) on some occasions. Typically such speeds occurred in bursts of variable duration associated with periods of high winds. In order to assess surface gravity wave effects, we collected data at this depth in burst mode at 25 Hz every 3 hours using a Sontek Hydra current meter. There are a few episodes where the observed wave-induced motions are significant (>0.2 m s^{-1}). For example, on day 252 the observed wave-induced motions were >0.3 m s^{-1} at 0.75 m above the bottom. When this is compared to the maximum mean currents of 0.14 m s^{-1}, there is a possibility for wave-current interactions during these episodes. On several occasions mean bottom currents flowed in the opposite direction to the surface currents because of the surface pressure gradient due to wind setup in the basin. In general, the vertical velocities in the thermocline and the hypolimnion were directed upward, whereas in the epilimnion they were directed toward the bottom. On day 252, strong vertical currents (-0.025 m s^{-1}) were observed coinciding with the thermocline depression. In 2005, surface currents were marginally stronger than in 2004 and responded to the prevailing winds. As observed previously by Boyce and Chiocchio (1987), a striking feature of these current observations is the dominance of inertial oscillations coinciding with stronger winds in the sub-surface layer (Fig. 4e). The observed inertial currents are stronger in and above the thermocline region. We will further explore the effect of these short period oscillations in vertical and horizontal turbulent exchanges in the following sections.

Auto and rotary spectra have been calculated for all depths in both years. Spectra were computed using the fast Fourier transform method. All spectra were computed from multiple, overlapping, unfiltered data subsets of 128 hourly values, which were first transformed and then ensemble averaged and smoothed by Hanning filter. Furthermore, to determine if the peaks in the spectra are significant against a background spectrum, a red noise spectrum of univariate lag-1 autoregressive process was utilized (Percival and Walden 1993). The 90% confidence levels were obtained by multiplying the background spectrum by the 90 percentile value of χ^2_2-distribution. Figure 5a–c shows typical energy spectral density plots of temperature and rotary spectra of currents at selected depths in 2004. The spectral peak of temperature (Fig. 5a) is around 24 h and corresponds to diurnal variation. The secondary peak appears to be close to the inertial period (18 h $\sim$ 0.055 cph) and dominant in the sub-surface levels. The effects of the seasonal warming can be seen in the low frequency band (time scales longer than 1 day). The rotary spectra of currents (Fig. 5b,c) show several peaks. The clockwise spectrum of surface currents shows two significant peaks, one at 24 h and a secondary peak at 14.2 h (0.07 cph). The peak at 14.2 h appears to be the dominant peak in the counterclockwise spectrum also. Saylor and Miller (1987) found a similar peak in their analysis and attributed it to the fundamental longitudinal seiche of the lake. The clockwise spectra of surface currents also show a peak close to 9.6 h (0.104 cph), indicating the presence of secondary longitudinal mode at this site. The sub-surface currents are dominated by inertial oscillations, which are clearly evident in the clockwise spectrum. The inertial peak, around 18 h, is inherent to all sub-surface depths, and this peak decreases in the hypolimnion. The mixed layer is predominantly driven by wind and inertial forces, whereas the hypolimnion derives its energy from large-scale wind forcing. In 2005 the dominant peak is due to inertial oscillations at 15-m depth (Fig. 5d). Although the spectral energy levels were slightly higher in 2005 than in 2004, similar characteristics were obtained (Fig. 5e,f). The energy falls quite rapidly in the high frequency band (0.1–0.5 cph). Rao and Murthy (2001*a*) noted that these fluctuations are not entirely random in this band but they contribute to dispersal processes; hence, they are included in fluctuating turbulent currents. Boyce and Chiocchio (1987) also noted that the currents in this range are due to large-scale turbulence. However, they did not quantify the horizontal turbulence in their study. Consequently, we use a low-pass filter with a cut-off periodicity of 8–10 h to filter out all high-frequency oscillations from the mean flow.

Horizontal mixing

In large lakes horizontal mixing is a consequence of both fluctuations of the velocity field and the shear in the advective fields. Most experimental investigations on horizontal mixing were made with artificial tracers or drifters (Murthy 1976; Peeters et al. 1996). On the other hand, long time series of horizontal current fluctuations at fixed points obtained from moored current meters can also be interpreted in terms of mixing parameters (Lemmin 1989; Rao and Murthy 2001*a*). Royer et al. (1987) also observed that small scale fluctuations contribute to horizontal variability of temperature in the central basin. In order to estimate horizontal exchange coefficients in the mid-central basin of Lake Erie, we use current velocity data obtained from both ADCP and Sontek Hydra stations. An analysis of the entire temperature and current time series in each year will reveal an average flow regime for the duration of the whole record in response to the associated synoptic wind forcing. The time series of low frequency (filtered, >8 h) flow values in the previous section $\bar{u}(t)$ and $\bar{v}(t)$ are subtracted from the observed hourly values $u(t)$ and $v(t)$ to obtain the fluctuations $u'(t)$ and $v'(t)$. The variance ($\overline{u'^2}$ and $\overline{v'^2}$) is used as a measure of the magnitude of velocity fluctuations. Here, the overbar in the variance represents time averaging from day 211 to day 280 for late summer conditions.

The intensity of horizontal turbulence is calculated as the ratios

$$[i_u, i_v] = \left[\frac{\sqrt{\overline{(u')^2}}}{\sqrt{(\bar{u})^2 + (\bar{v})^2}}, \frac{\sqrt{\overline{(v')^2}}}{\sqrt{(\bar{u})^2 + (\bar{v})^2}}\right] \qquad (1)$$

which measure the magnitude of turbulent pulsations relative to the mean flow velocity.

The mean flow kinetic energy (MKE), and the fluctuating (turbulent) currents kinetic energy (TKE) are then simply given as

$$\{\mathrm{MKE}, \mathrm{TKE}\} = \left\{\frac{1}{2}\left(\overline{\bar{u}^2} + \overline{\bar{v}^2}\right), \frac{1}{2}\left(\overline{u'^2} + \overline{v'^2}\right)\right\} \qquad (2)$$

Rao and Murthy (2001*a*) developed a relationship using Taylor's (1921) analysis between the horizontal exchange coefficient and the Eulerian current fluctuations in Lake Ontario. In their study, the horizontal exchange coefficient

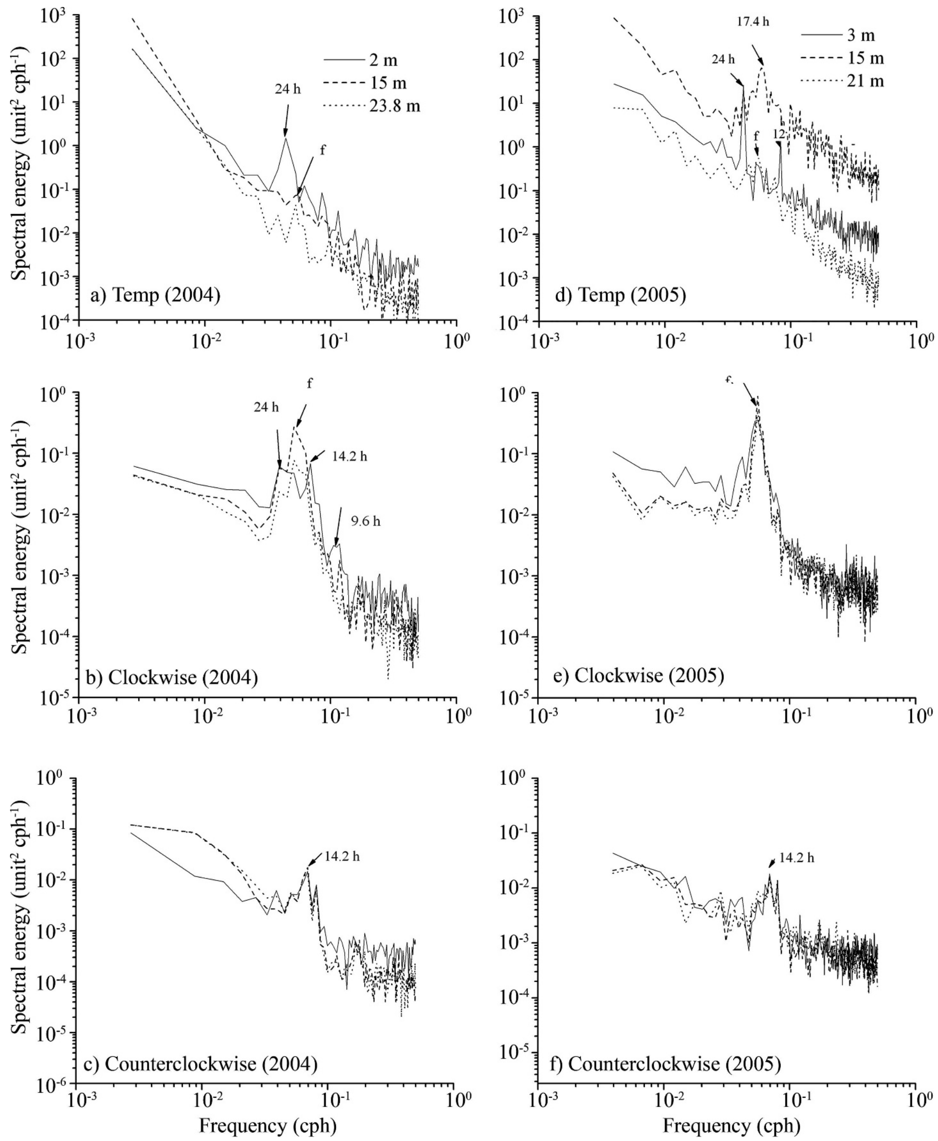

Fig. 5. Temperature and rotary current spectra at three depths for the summers of 2004 and 2005 deployments: (a) temperature (2004), (b) clockwise (2004), (c) counterclockwise (2004), (d) temperature (2005), (e) clockwise (2005), and (f) counterclockwise. Arrows indicate peaks above the 90% confidence spectrum, f is inertial period.

(K) in terms of Eulerian statistics was written as

$$K = \beta \overline{u'^2} \tau \tag{3}$$

where $\tau = \int_0^\infty R(\tau)\, d\tau$ is the Eulerian integral time scale and $R(\tau)$ is the Eulerian auto-correlation coefficient. Schott and Quadfasel (1979) have determined values of β to the order of 1.4 ± 0.4 based on simultaneous Lagrangian and Eulerian measurements in the Baltic Sea, which was also confirmed in Lake Ontario (Rao and Murthy 2001*a*). In the absence of simultaneous Lagrangian measurements, we have chosen $\beta = 1.4$ as a mean value for the present study to estimate the horizontal exchange coefficients in Lake Erie.

Graphs of the components of mean currents, turbulence intensity, kinetic energy, and horizontal mixing coefficients as a function of depth are shown in Fig. 6a–d for 2004 and 2005. The synoptic mean flow direction is toward the southwest with increased velocity at mid-depth in 2004. In 2005, although the surface currents flowed toward east-southeast, the currents from mid-depths were in opposite direction. These characteristics coincided with the strong stratification at those depths. To determine if time averaging affected the observed vertical structure, time average profiles were computed over periods of 8 days (typical period of large-scale circulation in the lake). This also yielded similar profiles as shown in these mean summer profiles in 2004 and 2005. Thus the basic vertical structure did not vary substantially within the year, but significant differences were observed between the years. These differences were due to the prevailing winds and the position of the thermocline. Csanady (1984) predicts

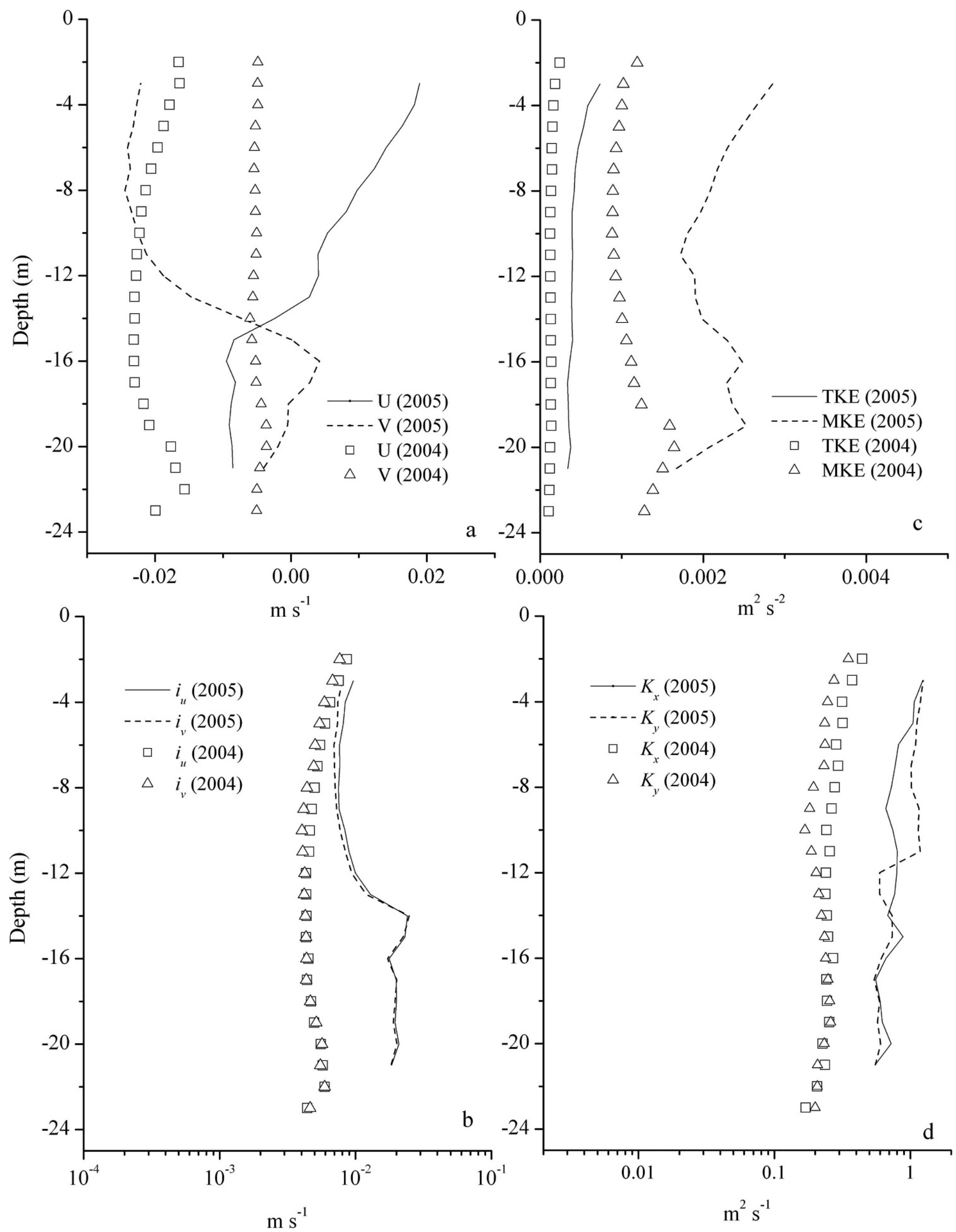

Fig. 6. (a) Mean east–west and north–south currents, (b) turbulence intensity coefficients, (c) components of kinetic energy (mean flow and turbulent), and (d) horizontal exchange coefficients during the summers of 2004 and 2005.

coastal flows parallel to the wind and a return flow in the deeper waters. This is clearly evident from 2005 measurements, which show that currents in the thermocline and hypolimnion flowed in opposite direction to the wind because of the surface pressure gradient (Boyce and Chiocchio 1987). The turbulence intensity coefficients were nearly isotropic during both years, however, the magnitudes were higher at sub-surface and below in 2005 (Fig. 6b). This is also evident in the kinetic energy levels during these years (Fig. 6c). The MKE was generally higher than TKE during the summer. The MKE levels in 2005 also showed significant shear in the upper water column.

Plots of the horizontal exchange coefficients, K_x and K_y, as a function of depth are shown in Fig. 6d. In general the east–west (K_x) exchange coefficients were higher in the surface layer (0.5 $m^2\ s^{-1}$) in comparison to north–south (K_y) exchange coefficients (0.35 $m^2\ s^{-1}$) in 2004. However, below the surface mixed layer the magnitude of both the components are comparable. Between the days 251 to 253 the east–west horizontal exchange coefficients increased to 0.6 $m^2\ s^{-1}$, whereas the north–south component increased to 0.82 $m^2\ s^{-1}$ in the thermocline region. In general, horizontal exchange coefficients were also higher in 2005 and increased marginally during the change point (days 242–243). In both years horizontal exchange coefficients decreased with depth. Murthy (1972) reported that in the hypolimnion of the central basin, the horizontal diffusion coefficients are on the order of 0.1 $m^2\ s^{-1}$. In other lakes, for example in Swiss lakes, Peeters et al. (1996) obtained horizontal diffusivities in the range of 0.2 $m^2 s^{-1}$ to 0.3 $m^2 s^{-1}$. Rao and Murthy (2001*b*) also showed that horizontal exchange coefficients in the coastal waters of Lake Ontario varied between 0.02 $m^2 s^{-1}$ to 2.0 $m^2 s^{-1}$ during summer. The general range of horizontal exchange coefficients (0.2–1.2 $m^2 s^{-1}$) obtained in this study is, therefore, comparable to these observations.

Vertical mixing

Several mechanisms such as current shear, breaking of internal waves, or convective overturns contribute to the generation of vertical turbulence in lakes. The strong influence that the vertical shear and stability have on turbulence can be estimated from the gradient Richardson number, $Ri = N^2/S^2$. Here, N is the Brunt-Vaisala frequency given as $N^2 = -(g/\rho_0)(\partial\rho/\partial z)$ and the vertical current shear $S^2 = (\partial u/\partial z)^2 + (\partial v/\partial z)^2$, where z is the vertical coordinate positive upward; u and v are hourly east–west and north–south currents, respectively; g is the acceleration due to gravity, and ρ_0 is reference density. The density of the lake water was estimated from the temperature data from thermistor moorings and calculated according to Chen and Millero (1986) formula. The temperature data at different levels were smoothly interpolated using a cubic spline technique to match with ADCP current measurement levels.

The turbulent mixing can be calculated on the basis of different models using advanced turbulence closure schemes. However, in this study following Rao and Murthy (2001*b*), we employ a simple empirical formula suggested by Pacanowski and Philander (1981). They related the eddy diffusivity (K_z) to the Richardson number and studied the modeling of temperature structure in the tropical ocean, which is given as

$$K_z = \frac{K_o}{(1 + 5Ri)^2} + K_b \tag{4}$$

where K_o is an adjustable parameter and K_b is the background eddy diffusivity. In the present study following Omstedt and Murthy (1994), we assign $K_o = 10^{-2}$ $m^2 s^{-1}$ and $K_b = 10^{-7}$ $m^2 s^{-1}$ to account for low eddy diffusivity values in the Great Lakes. Similar parameterization of vertical mixing in terms of Richardson number has been used in several studies (Rao et al. 2004; Loewen et al. 2007). The eddy diffusivity coefficients calculated by Eq. 4 are not quite complete, as K_z becomes constant under homogeneous conditions. Given the uncertainties, the K_z values obtained here should be considered only as an order of magnitude estimates.

Figure 7a–c shows the time series of Brunt-Vaisala frequency (N), vertical shear (S^2), and eddy diffusivity (K_z) obtained by Eq. 4 in 2004. During the stratified period from day 211 to day 262, the main thermocline was below 15 m where N values were high (>0.04 s^{-1}). The Brunt-Vaisala frequency values were also slightly higher at 10 m because of secondary thermocline from day 211 to day 229. The Brunt-Vaisala frequency in the surface layer (<8 m) exhibited diurnal signal throughout the deployment. A similar diurnal cycle of N values can be noticed between 10 m and 11 m; however, the temperature difference between these depths was found to be 0.05 ± 0.09°C (max = 0.61°C). These temperature differences are small and have not shown significant effect on vertical mixing. In the rest of the water column N values were small. Comparison of the time series of wind stress (Fig. 2a) and vertical current shear (Fig. 7b) shows that current shear in the upper mixed layer was closely related to the east–west component of wind stress. In the hypolimnion the mean currents were high, providing conditions for strong shearing stress in that layer. Because of this, Richardson numbers were at near critical values (<0.25) producing high vertical eddy diffusivity values. Just above the thermocline, because of low values of Brunt-Vaisala frequency and current shear due to near-inertial oscillations, the turbulence was enhanced, thus increasing the vertical eddy diffusivity coefficients (0.0003–0.0005 $m^2 s^{-1}$). In the rest of the water column vertical shear was moderate. The strong eastward wind event from day 252–253 shifted the thermocline to deeper levels. Although the vertical current shear due to inertial oscillations was considerably high in the thermocline region, it was not sufficient to overcome the stable stratification in the thermocline. The thermocline was sharply defined from day 253 to day 263, thus increasing N (~0.05 s^{-1}) just above the hypolimnion. Because of the combined effects of radiative and turbulent heat losses and high winds from day 264, the Brunt-Vaisala frequency reduced to small values, enhancing the mixing throughout the water column.

Figure 8a–c shows the time series of Brunt-Vaisala frequency (N), vertical shear (S^2), and eddy diffusivity (K_z) in 2005. The vertical current shear was strong above the thermocline because of near-inertial oscillations, and the current shear in the thermocline increased following strong winds. Between days 214 and 225 the thermocline was thick, and appreciable current shear was observed due to inertial motion. In particular, the shear-induced motions from days 222–223 were responsible for mixing of thermocline waters and subsequent warming of the hypolimnion. The vertical eddy diffusivity coefficients during this period are comparable to 2004 values; however, the variability over depth and time is considerably different. These differences are due to differences in the prevailing winds and surface heat fluxes during this year. In general the turbulent exchange coefficients varied between 1×10^{-5} to 1×10^{-4} $m^2 s^{-1}$ with higher values near the surface and close to the bottom. The range of these values is consistent with limited observations using tracer (Murthy 1972) and microstructure probe in the central basin (Edwards et al. 2005).

Implications for dissolved oxygen concentration in the hypolimnion

Charlton and Milne (2004) provided a summary of dissolved oxygen (DO) data from the lake-wide surveillance cruises from 1990–2000. They showed that the mean DO

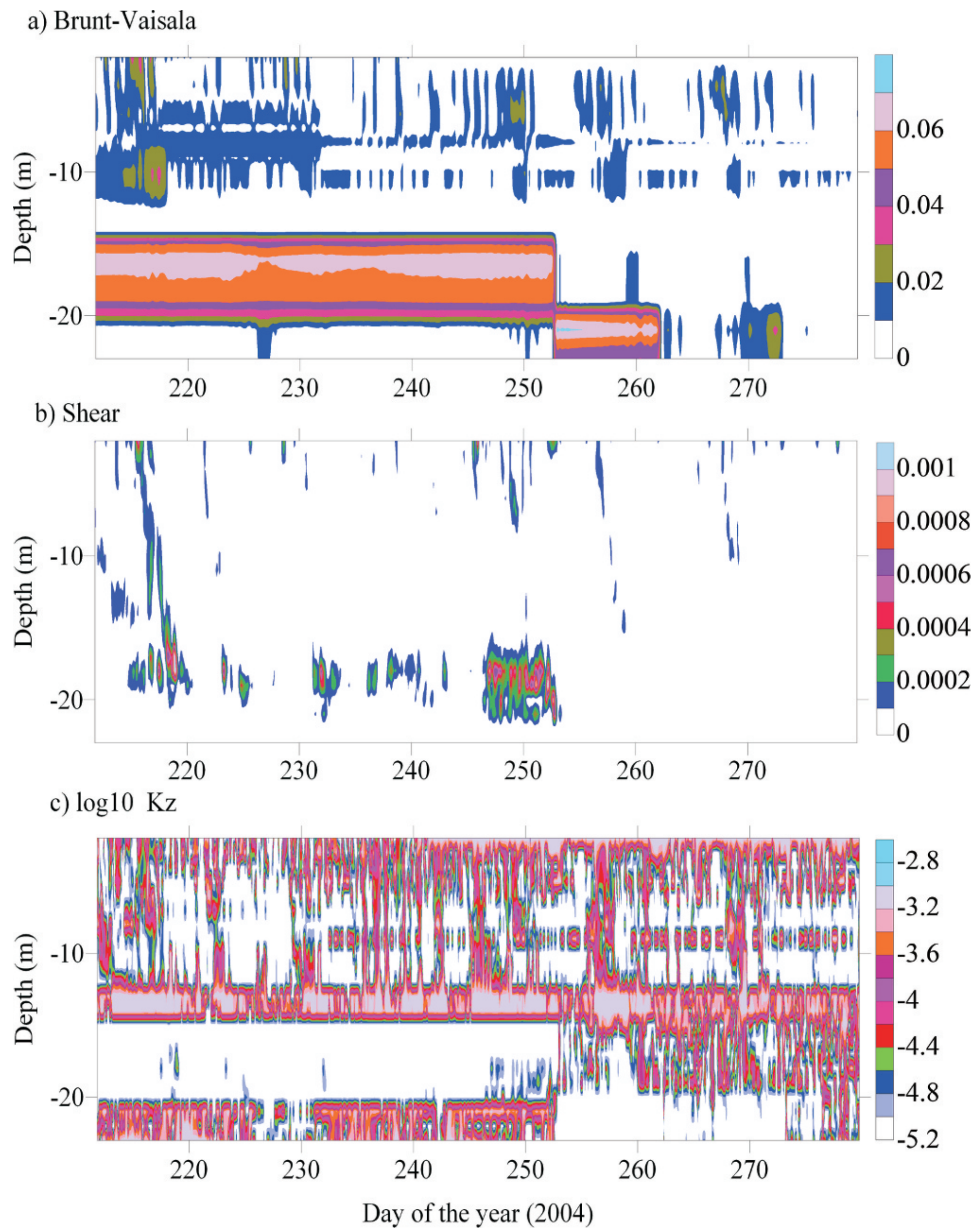

Fig. 7. The time series of (a) Brunt-Vaisala frequency (N) in s^{-1} (b) Shear (S^2) in s^{-2}, and (c) vertical eddy diffusivity, $\log_{10}(K_z)$ in $m^2\ s^{-1}$ during the summer of 2004.

depletion rates in the hypolimnion of the central basin varied between 0.13 mg L^{-1} d^{-1} to 0.07 mg L^{-1} d^{-1}. Figure 9 shows the DO concentrations and hypolimnion thickness from all central basin surveillance cruise data during 2004. Significant spatial variability can be observed in both DO and hypolimnion thickness. As noted in previous studies (Charlton and Milne 2004 and references therein) the highest depletion rates corresponded with the thinnest hypolimnion. The DO depletion rate from the measurements shown in Fig. 9 is 0.077 mg L^{-1} d^{-1}, which is in the range of previous observations. In order to study the processes responsible for short-term DO variability we used time series data from moored instruments. In 2004, two YSI6600 EDS systems containing oxygen and turbidity sensors were deployed at two depths, one in the epilimnion (12.3 m) and the other in hypolimnion (23.7 m), close to the other moorings (Fig. 10a). The accuracy of DO measurements in both years was verified by shipboard Winkler titration of water samples collected during the surveillance cruises. The DO concentrations in the epilimnion showed diurnal variability but in general remained between 8 mg L^{-1} and 9.5 mg L^{-1} during this period. In the hypolimnion, the concentrations decreased from 6 mg L^{-1} on day 211 to hypoxic levels (2 mg L^{-1}) by day 240. Further DO depletion occurred slowly until day 253; after that the DO depletion was rapid, and the water became close to anoxic. Between days 211 and 258 the depletion rate was around -0.12 mg L^{-1} d^{-1}, however,

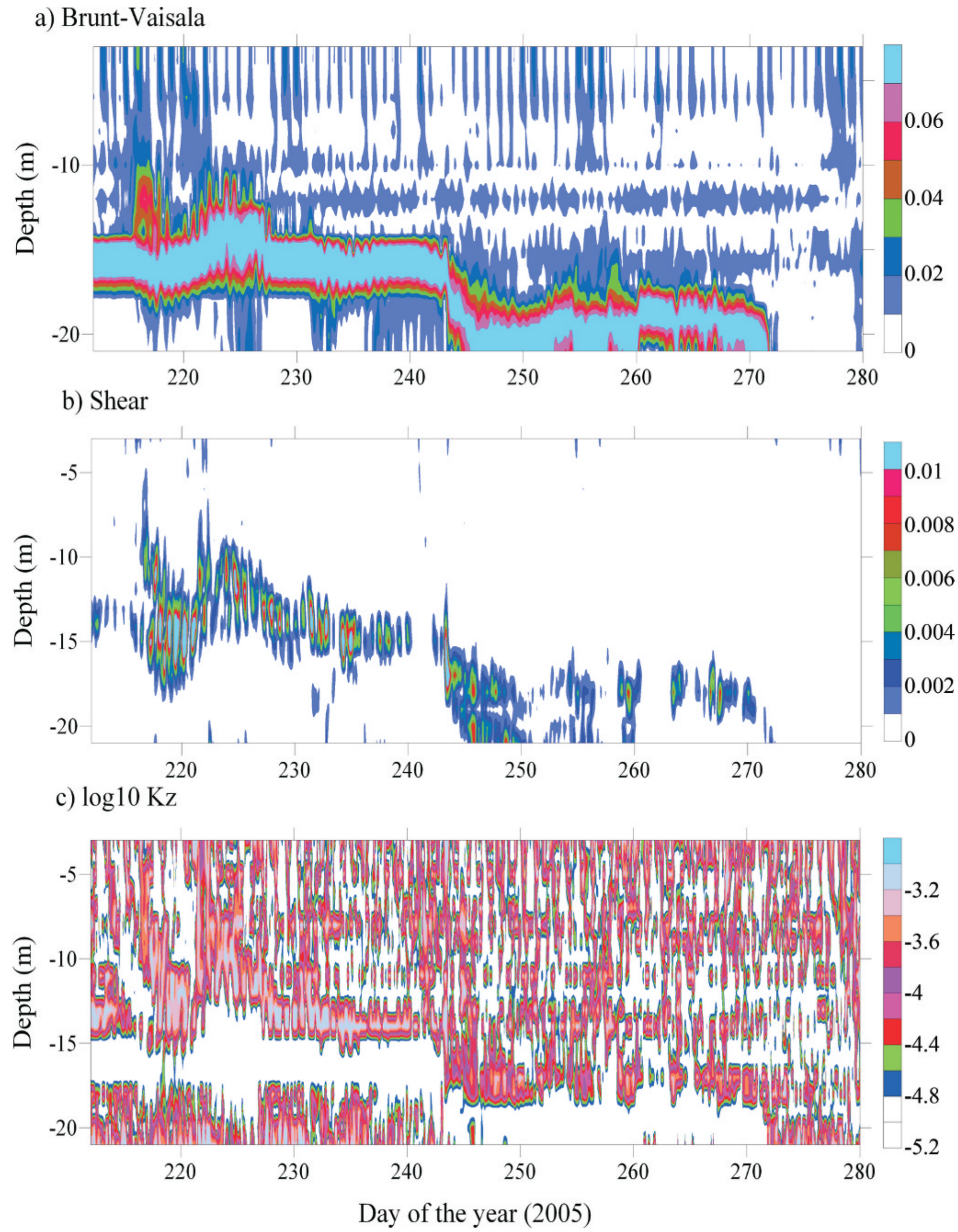

Fig. 8. The same as Fig. 7 except for the summer of 2005.

significant short-term changes between +0.87 mg L^{-1} d^{-1} and -1.16 mg L^{-1} d^{-1} were observed.

The seasonal depletion of DO in the hypolimnion is caused by the combination of the sediment oxygen demand (SOD) and water column oxygen demand. Values of SOD measured by Snodgrass (1987) and Charlton (1980) in the central basin ranged from 0.07 mg L^{-1} d^{-1} to 0.035 mg L^{-1} d^{-1} for a 4-m-thick hypolimnion. More recently, Matisoff and Neeson (2005) estimated that SOD rate in the central basin was 0.080 $\pm$ -0.026 mg L^{-1} d^{-1} in a 3–5-m-thick hypolimnion. The SOD probably explains the steady decrease of DO concentrations on a seasonal scale, but it cannot account for the rapid variability of DO at this location.

While the shallow depth of the hypolimnion is an important factor for DO budget, several other factors influence the change of DO concentration in the water column. The physical processes presented earlier will strongly influence the DO concentrations in the hypolimnion. Royer et al. (1987) showed that physical and transport processes produce significant changes of hypolimnion characteristics at short time scales (hours to days). These factors are crucial for delaying the setting of anoxia in the central basin. Ivey and Patterson (1982) and Patterson et al. (1985) developed a one-dimensional oxygen budget model for the central basin of Lake Erie. Lam and Schertzer (1987) also used a similar approach for studying the relationship of anoxic conditions in Lake Erie. More recently, a similar one-

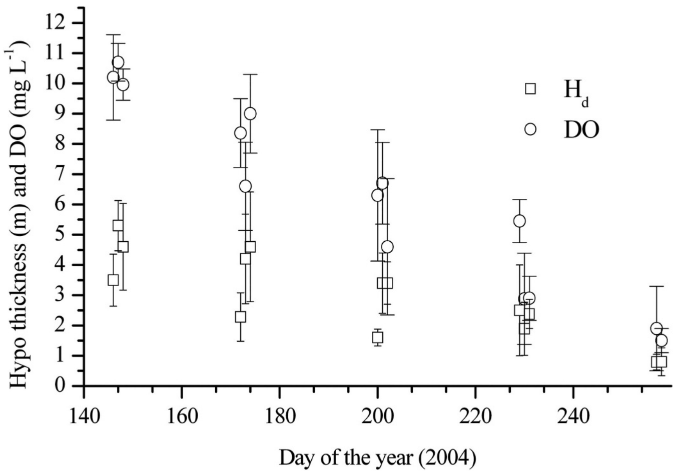

Fig. 9. Hypolimnion thickness and dissolved oxygen in the hypolimnion from 2004 surveillance observations.

dimensional model has been used by Edwards et al. (2005). All these studies are based on lake-wide surveillance data and showed that turbulent mixing plays a major role in the oxygen distribution in the hypolimnion of the central basin. As suggested by these authors, by ignoring horizontal transport and mixing, a one-dimensional mass conservation balance for DO in the hypolimnion can be written as

$$\frac{dO_h}{dt} = \frac{K_z}{H_d}\left(\frac{O_e - O_h}{\Delta z}\right) - (\mathrm{SOD} + P - R) \qquad (5)$$

where O_e and O_h are oxygen concentrations in epilimnion and hypolimnion, respectively, Δz is the thermocline thickness, K_z is the eddy diffusivity obtained using Eq. 4, SOD is sediment oxygen demand, and P and R are hypolimnion oxygen production and respiration. In Fig. 10b we show the hypolimnion thickness at the mooring (H_d), oxygen variation per day (term 1 in Eq. 5), and DO flux to the hypolimnion (term 2 in Eq. 5) as observed during this period. The hypolimnion thickness was around 4 m until day 252 and thereafter decreased to 0.8 m and remained

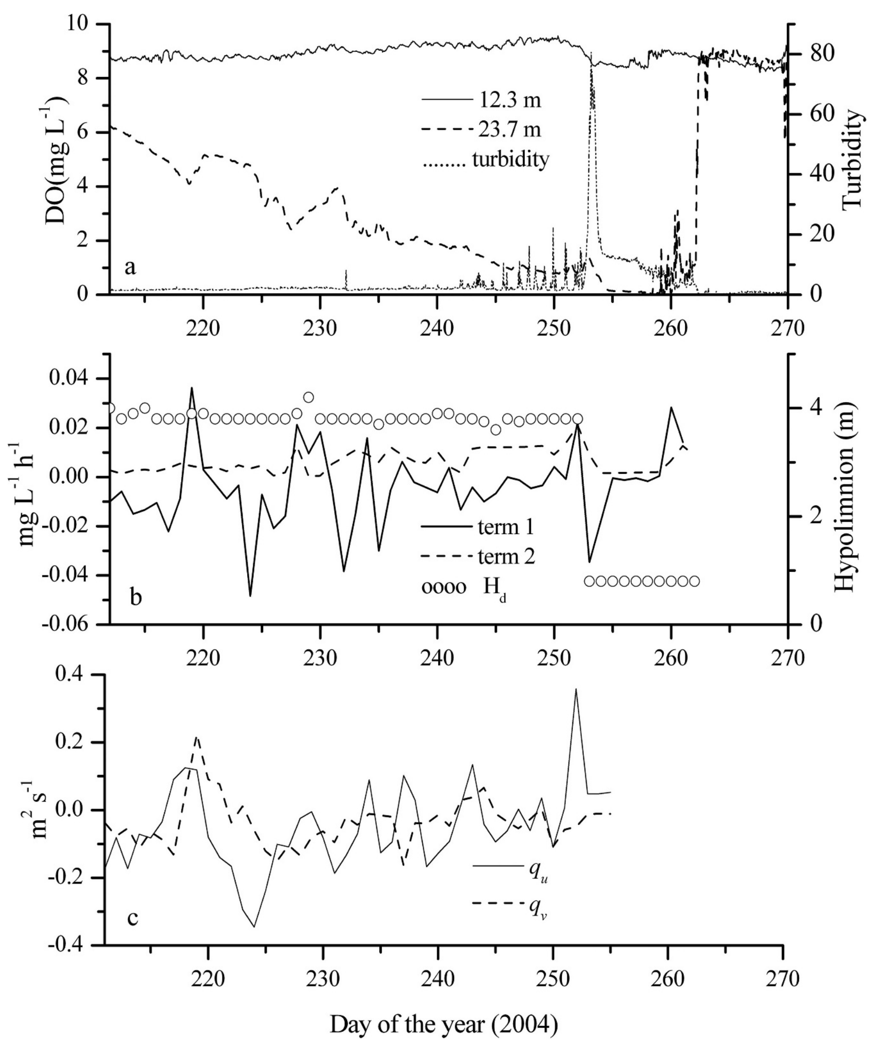

Fig. 10. (a) The time series of observed dissolved oxygen (left axis) and turbidity (right axis) from YSI mooring in the central basin during 2004; (b) terms in Eq. 5; and (c) horizontal transport in the hypolimnion.

there until the lake overturned. The small changes in the hypolimnion thickness coincided with wind-induced vertical mixing. The DO depletion varied quite rapidly within this period. The DO flux due to turbulent mixing appears to balance observed oxygen variability only on certain episodes. For example, the increased turbulence due to clockwise rotating winds on day 219 contributed only marginally to the increased oxygen at this location. The turbulent mixing balances the oxygen variation on day 235 and played a major role during the strong wind event on day 252. As suggested in previous studies these results also indicate that the variability of oxygen concentrations in the hypolimnion on occasions is due to the downward mixing of oxygen. In general the hypolimnion depth alone, which was already thin ($\sim$4 m), did not show a significant effect on the short-term variability of DO until day 252. Lam and Schertzer (1987) suggested that anoxia develops when the hypolimnion layer is $<$4 m and vertical diffusion is low (1×10^{-4} m^2 s^{-1}). Although the turbulent diffusivity below the thermocline was low ($<1 \times 10^{-4}$ m^2 s^{-1}) from day 211 to day 252, this did not result in immediate anoxic conditions. Shortly after day 253 the hypolimnion thickness dropped to 0.8 m, and strong stable stratification ($N > 0.05$ s^{-1}) was observed in the thermocline. Although this had considerable effect on oxygen depletion and the hypolimnion layer at this location, significant resuspension of bottom sediments would have also played a major role in the rapid decrease in oxygen concentrations on day 253. The bottom sediments in the central basin generally have a higher percentage of easily oxidizable substances that consume oxygen when exposed (Davis et al. 1987). Such resuspension of bottom sediments can be clearly seen in the turbidity peak caused by the strong easterly wind episode at this location (Fig. 10a). Bottom stresses on this day (calculated from the current and wave parameters using the method of Li and Amos 2002) exceeded 0.3 Pa, well above the stress needed to initiate bottom resuspension at this site (Lick et al. 1994). As mentioned before, SOD (term 3 in Eq. 1) is responsible for the gradual decrease of DO concentrations in the hypolimnion, but it cannot account for the rapid variability of DO concentrations.

The significant DO variability observed from day 211 to 225 could also be due to the horizontal flux of oxygen because of horizontal mixing and transport past the mooring. The mean horizontal exchange coefficients in the hypolimnion were about 2×10^{-1} m^2 s^{-1}. The typical oxygen concentration gradient in the central basin from the surveillance cruises was 5×10^{-5} mg L^{-1} m^{-1}. This will cause a diffusive flux in the order of 10^{-2} mg m^{-2} s^{-1} at this location. Therefore it is evident that vertical mixing and the horizontal mixing together are not sufficient to balance the observed short-term oxygen variation at this station. In order to verify if horizontal transport played a significant role in the observed DO variability, we have approximated the mean transport in the hypolimnion as

$$q_u = \int_0^{H_d} u\, dz, \qquad q_v = \int_0^{H_d} v\, dz \qquad (6)$$

Figure 10c shows the east–west (q_u) and north–south (q_v) components of transport in the hypolimnion during this period. It is clear that the sudden increase in oxygen levels on day 219 was due to the northwest transport of water from shallow layers. The vertical velocities during this episode were small and positive, therefore, entrainment of thermocline waters into the hypolimnion is not significant. The significant drop in oxygen levels on day 224 also coincided with the transport from the surrounding less oxygenated waters. Figure 11 shows observations of DO concentrations and physical processes during the 2005 deployment period. During this period DO concentrations in the epilimnion were only available from the ship-board profiler, whereas DO concentrations in the hypolimnion were measured by a YSI 6600 EDS sonde at 23 m. It was evident from 2004 measurements that DO concentrations do not vary significantly in the epilimnion; therefore, we use a linear interpolation to fill the missing data in that layer. In general, variability of DO concentrations and its relation to physical processes are similar to 2004 observations. These results support the view that in the hypolimnion the heat and DO variability are affected by the horizontal transport (Royer et al. 1987).

Discussion

The Eulerian data during the summers of 2004 and 2005 in the central basin of Lake Erie show significant variability of currents and temperature because of differences in the forcing conditions between the years. The mean currents throughout the water column were directed toward the southwest in 2004, whereas they showed a two-layer structure in 2005. As reported in previous studies, our results also suggest that the near-surface currents are wind-driven, whereas the hypolimnion motions are mainly because of surface pressure gradient due to wind setup. In both years the current and temperature spectra showed a prominent peak at around 18 h, indicating the presence of clock-wise rotating inertial waves. Although the peak energy at the high-frequency end was located mainly at the near-inertial frequency band, significant energy was observed at much smaller scales, indicating the presence of longitudinal seiche motions.

The horizontal exchange characteristics of the water column are parameterized with two horizontal exchange coefficients for momentum (K_x and K_y). The turbulence intensity coefficients indicate near-isotropy of horizontal turbulence in the hypolimnion during both 2004 and 2005. The MKE was generally higher than TKE during the summer. The east–west horizontal exchange coefficients were marginally higher (0.5 m^2 s^{-1}) than north–south exchange coefficients (0.35 m^2 s^{-1}) in the epilimnion.

Detailed observations of currents and temperatures during these years are used to study the relationship between vertical current shear and stratification. This study has demonstrated that the processes controlling the vertical mixing vary both between and within different water layers. In general the largest shear was observed above or sometimes in the thermocline and close to the bottom. Its magnitude varied with time following changes in wind-stress characteristics. Inertial shear dominated after strong

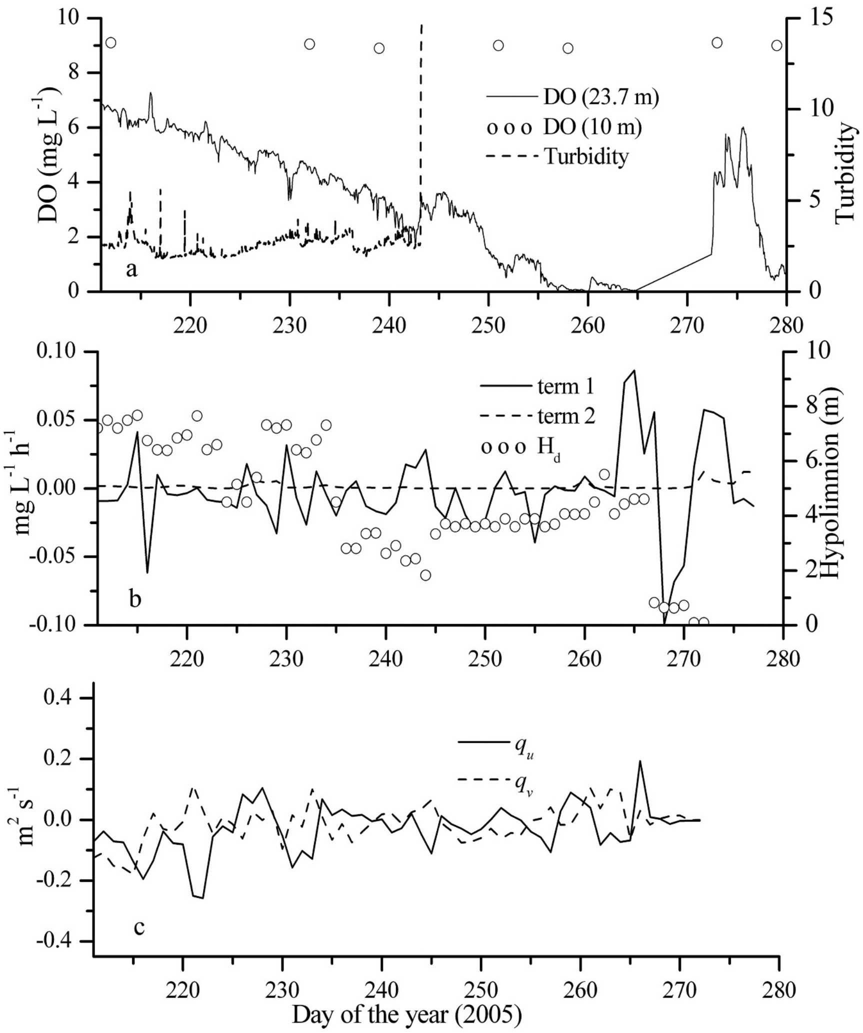

Fig. 11. The same as Figure 10 except for the summer of 2005.

winds when the thermocline was thick in 2004 and in the early part of 2005; however, when the thermocline was thin the high vertical current shear was noticed in the surface layer. Vertical exchange coefficients (K_z) were obtained by calculating Richardson numbers in the water column. The general range of K_z varied from 1×10^{-5} to 1×10^{-4} m^2 s^{-1}. The high values are usually noticed in the surface layer associated with strong shear and weak stratification. In both years the high values are also observed just above the thermocline and near the bottom due to enhanced vertical shear and reduced Brunt-Vaisala frequencies. The range of K_z values during the late summer conditions were comparable to the typical values obtained by Murthy (1972) and more recently by Edwards et al. (2005) in Lake Erie.

Although eutrophication is a contributor to hypolimnetic hypoxia, physical factors play a major role in dissolved oxygen budget (Charlton 1980). The lake-wide surveillance data show strong spatial variability of both hypolimnion thickness and dissolved oxygen concentrations in the central basin. In general, the hypolimnion thickness decreased during the summer coinciding with decreasing DO concentrations in the hypolimnion. Ivey and Boyce (1982) suggested that the changes in hypolimnetic thickness were due to entrainment of thermocline waters into the hypolimnion caused by shearing stresses at the bottom. The vertical velocity measurements from the ADCPs provided limited support for such vertical transport mechanism in 2004 and 2005, whereas previously neglected wave-induced orbital motions appear to play a significant role in generation of shearing stresses during energetic wind events. The time series measurements of DO in the epilimnion and hypolimnion highlight the significance of physical processes in the short-term variability of DO in the hypolimnion. Although the mean depletion rate was around -0.12 mg L^{-1} d^{-1} between days 211 and 258, significant short-term changes between +0.87 and -1.16 mg L^{-1} d^{-1} were observed. The effect of hypolimnion thickness of 4 m was not significant on the short-term variability of DO in 2004. In certain strong wind conditions vertical mixing played a significant role in balancing the oxygen budget. The strong advective currents were sometimes responsible for sudden variations of DO concentrations in the hypolimnion. These measurements also show a resuspension event on day 253 and its importance in decreasing the DO concentrations in the hypolimnion. The sharp and persistent thermocline ($N > 0.05\ s^{-1}$) combined with shallow hypolimnion was responsible for the sustained anoxia at this location. The present study was based on 2-year high-resolution currents and temperature measurements in the vertical at one location; to confirm the spatial and temporal variability of these findings it is necessary to conduct these intensive studies at other selected sites in the central basin. However, these results further confirm the importance of physical processes and the need of proper incorporation of these processes in numerical models.

References

Boyce, F. M., M. N. Charlton, D. Rathke, C. H. Mortimer, and J. R. Bennett [eds.]. 1987. Lake Erie Bi-national Study 1979–1980. J. Great Lakes Res. Special Issue **13**.

———, and F. Chiocchio. 1987. Water movements at a mid-central basin site: Time and space scales, relation to wind and internal pressure gradients. J. Great Lakes Res. **13:** 530–541.

———, ———, B. Eid, F. Penicka, and F. Rosa. 1980. Hypolimnion flow between the central and eastern basins of Lake Erie during 1977 (Interbasin Hypolimnion Flows). J. Great Lakes Res. **6:** 290–306.

Burns, N. M., and C. Ross. 1972. Project Hypo, Paper No. 6, Canada Centre for Inland Waters, Burlington, Ontario. USEPA Tech. Report TS-05-71-208-24.

Charlton, M. N. 1980. Oxygen depletion in Lake Erie: Has there been any change? Can. J. Fish. Aquat. Sci. **37:** 72–81.

———, and J. Milne. 2004. Review of thirty years of change in Lake Erie water quality, NWRI Contribution No. 04-167. National Water Research Institute.

Chen, C. T. A., and F. J. Millero. 1986. Precise thermodynamic properties for natural waters covering only the limnological range. Limnol. Oceanogr. **31:** 657–662.

Csanady, G. T. 1984. Circulation in the coastal ocean. D. Reidel.

Davis, W. S., L. A. Fay, and C. E. Herdendorf. 1987. Overview of USEPA/CLEAR Lake Erie Sediment Oxygen demand investigations during 1979. J. Great Lakes Res. **13:** 731–737.

Edwards, W. J., J. D. Conroy, and D. A. Culver. 2005. Hypolimnetic oxygen depletion dynamics in the central basin of Lake Erie. J. Great Lakes Res. **31:** 262–271.

Hamblin, P. F. 1987. Meteorological forcing and water level fluctuations on Lake Erie. J. Great Lakes Res. **13:** 436–453.

Hawley, N., and others. 2006. Hypoxia in Lake Erie and The International Field Years for Lake Erie (IFYLE), EOS. Transactions of American Geophysical Union **87:** 313–319.

Ivey, G. N., and F. M. Boyce. 1982. Entrainment by bottom currents in Lake Erie. Limnol. Oceanogr. **27:** 1029–1034.

———, and J. C. Patterson. 1984. A model of the vertical mixing in Lake Erie in summer. Limnol. and Oceanogr. **29:** 553–563.

Lam, D. C. L., and W. M. Schertzer. 1987. Lake Erie thermocline model results: Comparison with 1987–1982 data and relation to anoxic occurrences. J. Great Lakes Res. **13:** 757–769.

———, ———, and R. C. McCrimmon. 2002. Modelling changes in phosphorus and dissolved oxygen pre- and post-zebra mussel arrival in Lake Erie, NWRI Contribution No. 02-198. National Water Research Institute.

Lemmin, U. 1989. Dynamics of horizontal mixing in the nearshore zone of Lake Geneva. Limnol. Oceanogr. **34:** 420–434.

Loewen, M. R., J. D. Ackerman, and P. F. Hamblin. 2007. Environmental implications of stratification and turbulent mixing in a shallow lake basin. Can. J. Fish. Aquat. Sci. **64:** 43–57.

Matisoff, G., and T. M. Neeson. 2005. Oxygen concentration and demand in Lake Erie sediments. J. Great Lakes Res. **31:** 284–295.

Murthy, C. R. 1972. An investigation of diffusion characteristics of the hypolimnion of Lake Erie, p. 39–44. *In* Project Hypo, Paper No. 6, Canada Centre for Inland Waters, Burlington, Ontario. USEPA Tech. Rept. TS-05-71-208–24.

———. 1976. Horizontal diffusion characteristics in Lake Ontario. J. Phys. Oceanogr. **6:** 76–84.

Omstedt, A., and C. R. Murthy. 1994. On currents and vertical mixing in lake Ontario during summer stratification. Nordic Hydrology **25:** 213–232.

Pacanowski, R. C., and S. G. Philander. 1981. Parameterization of vertical mixing in numerical models of tropical oceans. J. Phys. Oceanogr. **11:** 1443–1451.

Patterson, J. C., B. R. Allison, and G. N. Ivey. 1985. A dissolved oxygen budget model for Lake Erie in summer. Freshw. Biol. **15:** 683–694.

Peeters, F., A. Wuest, G. Piepke, and D. M. Imboden. 1996. Horizontal mixing in lakes. J. Geophys. Res. **101:** 18,361–18,375.

Percival, D. B., and A. T. Walden. 1993. Spectral analysis for physical applications. Cambridge Univ. Press.

Rao, Y. R., and C. R. Murthy. 2001*a*. Coastal boundary layer characteristics during summer stratification in Lake Ontario. J. Phys. Oceanogr. **31:** 1088–1104.

———, and ———. 2001*b*. Nearshore currents and turbulent exchange characteristics during upwelling and downwelling events in Lake Ontario. J. Geophys. Res. **106:** 2667–2678.

———, M. G. Skafel, and M. N. Charlton. 2004. Circulation and turbulent exchange characteristics during the thermal bar in Lake Ontario. Limnol. Oceanogr. **49:** 2190–2200.

Royer, L., F. Chiocchio, and F. M. Boyce. 1987. Tracking short-term physical and biological changes in the central basin of Lake Erie. J. Great Lakes Res. **13:** 587–606.

Saylor, J. H., and G. S. Miller. 1987. Studies of large-scale currents in Lake Erie, 1979–80. J. Great Lakes Res. **13:** 487–514.

Schertzer, W. M. 1987. Heat balance and heat storage estimates for Lake Erie, 1967 to 1982. J. Great Lakes Res. **13:** 454–467.

Schott, F., and D. Quadfasel. 1979. Lagrangian and Eulerian measurements of horizontal mixing in the Baltic. Tellus. **31:** 138–144.

Snodgrass, W. J. 1987. Analysis of models and measurements for sediment oxygen demand in Lake Erie. J. Great Lakes Res. **13:** 738–756.

Taylor, G. I. 1921. Diffusion by continuous movements. Proc. London Math. Soc. **20:** 196–212.

Vollenweider, R. A. 1968. Scientific fundamentals of the eutrophication of lakes and flowing waters with particular reference to nitrogen and phosphorus as factors in eutrophication. Organization for Economic Co-Operation and Development. DAS/CSI/68.27.

Wu, J. 1980. Wind-stress coefficients over sea surface near neutral conditions—a revisit. J. Phys. Oceanogr. **10:** 727–740.

Received: 2 November 2006
Amended: 22 February 2008
Accepted: 2 April 2008